



CHORUS

This is the accepted manuscript made available via CHORUS. The article has been published as:

First Observation of P-odd γ Asymmetry in Polarized Neutron Capture on Hydrogen

D. Blyth *et al.* (NPDGamma Collaboration)

Phys. Rev. Lett. **121**, 242002 — Published 13 December 2018

DOI: [10.1103/PhysRevLett.121.242002](https://doi.org/10.1103/PhysRevLett.121.242002)

1 First Observation of P -odd γ Asymmetry in Polarized Neutron Capture on Hydrogen

2 D. Blyth,^{1,2} J. Fry,^{3,4} N. Fomin,^{5,6} R. Alarcon,¹ L. Alonzi,³ E. Askanazi,³ S. Baeßler,^{3,7} S. Balascuta,^{8,1}
3 L. Barrón-Palos,⁹ A. Barzilov,¹⁰ J.D. Bowman,⁷ N. Birge,⁵ J.R. Calarco,¹¹ T.E. Chupp,¹² V. Cianciolo,⁷
4 C.E. Coppola,⁵ C. B. Crawford,¹³ K. Craycraft,^{5,13} D. Evans,^{3,4} C. Fieseler,¹³ E. Frlež,³ I. Garishvili,^{7,5}
5 M.T.W. Gericke,¹⁴ R.C. Gillis,^{7,4} K.B. Grammer,^{7,5} G.L. Greene,^{5,7} J. Hall,³ J. Hamblen,¹⁵ C. Hayes,^{16,5}
6 E.B. Iverson,⁷ M.L. Kabir,^{17,13} S. Kucuker,^{18,5} B. Lauss,¹⁹ R. Mahurin,²⁰ M. McCrea,^{13,14} M.
7 Maldonado-Velázquez,⁹ Y. Masuda,²¹ J. Mei,⁴ R. Milburn,¹³ P.E. Mueller,⁷ M. Musgrave,^{22,5} H. Nann,⁴
8 I. Novikov,²³ D. Parsons,¹⁵ S.I. Penttilä,⁷ D. Počanić,³ A. Ramirez-Morales,⁹ M. Root,³ A. Salas-Bacci,³
9 S. Santra,²⁴ S. Schröder,^{3,25} E. Scott,⁵ P.-N. Seo,^{3,26} E.I. Sharapov,²⁷ F. Simmons,¹³ W.M. Snow,⁴ A. Sprow,¹³
10 J. Stewart,¹⁵ E. Tang,^{13,6} Z. Tang,^{4,6} X. Tong,⁷ D.J. Turkoglu,²⁸ R. Whitehead,⁵ and W.S. Wilburn⁶

11 (The NPDGamma Collaboration)

12 ¹Arizona State University, Tempe, AZ 85287

13 ²High Energy Physics Division, Argonne National Laboratory, Argonne, IL, 60439, USA

14 ³University of Virginia, Charlottesville, VA 22904, USA

15 ⁴Indiana University, Bloomington, IN 47405, USA

16 ⁵University of Tennessee, Knoxville, TN 37996, USA

17 ⁶Los Alamos National Laboratory, Los Alamos, NM 87545, USA

18 ⁷Oak Ridge National Laboratory, Oak Ridge, TN 37831, USA

19 ⁸Horia Hulubei National Institute for Physics and Nuclear Engineering, Magurele, Romania

20 ⁹Instituto de Física, Universidad Nacional Autónoma de México, Apartado Postal 20-364, 01000, México

21 ¹⁰University of Nevada, Las Vegas, NV 89154, USA

22 ¹¹University of New Hampshire, Durham, NH 03824, USA

23 ¹²University of Michigan, Ann Arbor, MI 48109, USA

24 ¹³University of Kentucky, Lexington, KY 40506, USA

25 ¹⁴University of Manitoba, Winnipeg, MB, Canada R3T 2N2

26 ¹⁵University of Tennessee, Chattanooga, TN 37403 USA

27 ¹⁶Physics Department, North Carolina State University, Raleigh, NC, USA

28 ¹⁷Mississippi State University, Mississippi State, MS 39759, USA

29 ¹⁸Northwestern University Feinberg School of Medicine, Chicago, IL 60611, USA

30 ¹⁹Paul Scherrer Institut, CH-5232 Villigen, Switzerland

31 ²⁰Middle Tennessee State University, Murfreesboro, TN 37132, USA

32 ²¹High Energy Accelerator Research Organization (KEK), Tsukuba-shi, 305-0801, Japan

33 ²²Massachusetts Institute of Technology, Cambridge, MA 02139, USA

34 ²³Western Kentucky University, Bowling Green, KY 42101, USA

35 ²⁴Bhabha Atomic Research Centre, Trombay, Mumbai 400085, India

36 ²⁵Saarland University, Institute of Experimental Ophthalmology,

37 Kurrberger Str. 100, Bldg. 22, 66424 Homburg/Saar, Germany

38 ²⁶Triangle Universities Nuclear Lab, Durham, NC 27708, USA

39 ²⁷Joint Institute for Nuclear Research, Dubna, Russia

40 ²⁸National Institute of Standards and Technology, Gaithersburg, MD 20899, USA

41 (Dated: November 7, 2018)

We report the first observation of the parity-violating gamma-ray asymmetry A_{γ}^{np} in neutron-proton capture using polarized cold neutrons incident on a liquid parahydrogen target at the Spallation Neutron Source at Oak Ridge National Laboratory. A_{γ}^{np} isolates the $\Delta I = 1$, ${}^3S_1 \rightarrow {}^3P_1$ component of the weak nucleon-nucleon interaction, which is dominated by pion exchange and can be directly related to a single coupling constant in either the DDH meson exchange model or pionless effective field theory. We measured $A_{\gamma}^{np} = (-3.0 \pm 1.4(\text{stat.}) \pm 0.2(\text{sys.})) \times 10^{-8}$, which implies a DDH weak πNN coupling of $h_{\pi}^1 = (2.6 \pm 1.2(\text{stat.}) \pm 0.2(\text{sys.})) \times 10^{-7}$ and a pionless EFT constant of $C^{3S_1 \rightarrow 3P_1}/C_0 = (-7.4 \pm 3.5(\text{stat.}) \pm 0.5(\text{sys.})) \times 10^{-11} \text{ MeV}^{-1}$. We describe the experiment, data analysis, systematic uncertainties, and implications of the result.

42 PACS numbers: 11.30.Er, 24.70.+s, 13.75.Cs, 07.85.-m, 25.40.Lw

43 *Introduction.* In this Letter we present the first ob- 47 the first determination of an isolated term in the weak
44 servation of the parity-violating (PV) asymmetry A_{γ}^{np} 48 nucleon-nucleon (NN) potential. This represents a ma-
45 of gammas emitted from the capture of polarized neu- 49 jor step toward a complete experimental determination
46 trons on protons. Analysis of the asymmetry leads to 50 of the spin-isospin structure of the hadronic weak inter-

action (HWI).¹⁰⁶

The electroweak component of the Standard Model¹⁰⁷ (SM) describes the weak couplings of W^\pm and Z gauge¹⁰⁸ bosons to quarks and, in principle, the HWI.¹⁰⁹ The HWI¹⁰⁹ causes parity-violating admixtures in nuclear wave func-¹¹⁰ tions and produces small, but observable, PV spin-¹¹¹ momentum correlations and photon circular polariza-¹¹² tions. However, nonperturbative QCD dynamics make a¹¹³ direct calculation of PV nuclear observables out of reach.¹¹⁴

Desplanques, Donoghue, and Holstein (DDH) [1] intro-¹¹⁵ duced a meson exchange model to describe the HWI. This¹¹⁶ model is parametrized by six parity-odd time-reversal-¹¹⁷ even rotational invariants that can be constructed from¹¹⁸ the spin, isospin, momenta, and coordinates of the inter-¹¹⁹ acting nucleons. Each term has a Yukawa dependence¹²⁰ in the separation of the nucleons with range determined¹²¹ by the mass of the exchanged meson (π , ρ , or ω). The¹²² six adjustable coupling constants are labeled by the me-¹²³ son exchanged and the change of the total isospin ΔI :¹²⁴ h_π^1 , $h_\rho^{0,1,2}$, and h_ω^1 . DDH also give reasonable ranges¹²⁵ for these coupling constants. Observables are calculated¹²⁶ as matrix elements of the PV potential terms between¹²⁷ nuclear states and the coupling constants are to be de-¹²⁸ termined from experiment.¹²⁹

The two-body $n - p$ system is exactly calculable once¹³⁰ the strong NN interaction is specified and there is no nu-¹³¹ clear structure uncertainty in the interpretation of A_γ^{np} .¹³² A_γ^{np} depends on only $\Delta I = 1$ coupling constants. Sim-¹³³ ilarly, the value of the circular polarization, P_γ , of the¹³⁴ 1.081 MeV γ emitted by unpolarized ^{18}F nuclei [2] de-¹³⁵ pends only on the $\Delta I = 1$ terms in the HWI. How-¹³⁶ ever, the contributions from heavy meson terms are much¹³⁷ larger in P_γ than in A_γ^{np} allowing a determination of h_π^1 ¹³⁸ and a linear combination of $\Delta I = 1$ heavy meson cou-¹³⁹ plings in a combined analysis.¹⁴⁰

New theoretical approaches to weak NN interactions¹⁴¹ based on effective field theory (EFT) and the $1/N_c$ ex-¹⁴² pansion of QCD, where N_c is the number of colors, pre-¹⁴³ dict relative sizes of PV couplings. In pionless EFT, the¹⁴⁴ HWI is described by five $S - P$ transition amplitudes¹⁴⁵ first introduced by Danilov [3] and elaborated in sub-¹⁴⁶ sequent work [4–7]. In the pionless EFT approach [7],¹⁴⁷ A_γ^{np} is proportional to the $\Delta I = 1$ low energy constant,¹⁴⁸ $C^3 S_1 \rightarrow ^3 P_1 / C_0$. Recently the $1/N_c$ expansion of QCD [8–¹⁴⁹ 12] has been applied to the HWI. Phillips *et al.* [13, 14]¹⁵⁰ constructed the $1/N_c$ expansion of the DDH couplings¹⁵¹ and Schindler *et al.* [15] have developed the $1/N_c$ ex-¹⁵² pansion in pionless EFT, valid for 2-body systems at low¹⁵³ energy, and the phenomenology was analyzed by Gardner¹⁵⁴ *et al.* [16]. In addition to $1/N_c$ dependence, all $\Delta I = 1$ ¹⁵⁵ terms in both DDH and EFT theories are suppressed by a¹⁵⁶ factor $\sin^2(\theta_W) = 0.223$. Since charged currents are sup-¹⁵⁷ pressed in $\Delta I = 1$ NN processes by $V_{us}^2/V_{ud}^2 = 0.053$, the¹⁵⁸ weak NN interaction is one of the few systems sensitive¹⁵⁹ to quark-quark neutral current effects [17, 18]. Within¹⁶⁰

each of the different theoretical approaches described¹⁶¹ above, predictions for the relative size of weak NN am-¹⁶² plitudes in different meson and isospin channels vary by¹⁶³ an order of magnitude. Their relative sizes may reveal¹⁶⁴ new aspects of strong QCD, and their calculation within¹⁶⁵ the SM has consequently been the subject of extensive¹⁶⁶ theoretical work [19–42, 68]. Finally, lattice gauge the-¹⁶⁷ ory calculations present an exciting intellectual opportu-¹⁶⁸ nity for understanding non-perturbative aspects of QCD.¹⁶⁹ Wasem [37] has published a pioneering lattice QCD cal-¹⁷⁰ culation of the contribution of connected diagrams to h_π^1 .

Experiment. We measured A_γ^{np} on the Fundamental¹⁷¹ Neutron Physics beamline (FnPB) at the Spallation Neu-¹⁷² tron Source (SNS) using the same apparatus as the first¹⁷³ phase of the experiment [43] with some improvements.¹⁷⁴ At the SNS proton pulses delivered at 60 Hz to a mer-¹⁷⁵ cury target produce spallation neutrons which are cooled¹⁷⁶ by a liquid hydrogen moderator. The neutrons travel¹⁷⁷ 15 m down a supermirror (SM) neutron guide [44] to the¹⁷⁸ NPDGamma experiment. Two choppers select neutron¹⁷⁹ wavelengths between 3.1-6.6 Å from each 60 Hz time-of-¹⁸⁰ flight (TOF) pulse and reject neutrons outside this range¹⁸¹ to prevent lower energy neutrons mixing into the next¹⁸² pulse. The neutron beam intensity was sampled by two¹⁸³ ^3He ionization chambers, one upstream (M1) and one¹⁸⁴ downstream (M4) from the hydrogen target [43, 45], see¹⁸⁵ Fig. 1. M1 absorbed approximately 1% of the beam and¹⁸⁶ determined the number of neutrons in each pulse with a¹⁸⁷ statistical uncertainty of 10^{-4} .

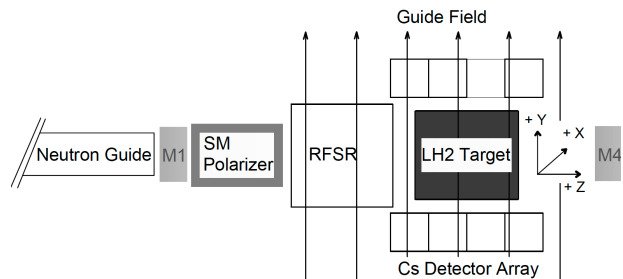


FIG. 1. A schematic vertical cut view of the NPDGamma experiment on the FnPB, for details see text.

After M1, neutrons passed through a SM polarizer and¹⁸⁸ emerged with an average polarization of 94% [46]. The¹⁸⁹ neutron spin was transported to the target by a uniform¹⁹⁰ magnetic field $\vec{B}_0 = 9.5$ G aligned within 3 mrad to the¹⁹¹ $+\hat{y}$ -axis. To eliminate Stern-Gerlach beam steering, the¹⁹² gradient was limited to $\partial B_y / \partial y \leq 2$ mG/cm within the¹⁹³ volume between the RF Spin Rotator (RFSR) and the¹⁹⁴ target volume [47, 48]. The neutron flux at the LH₂¹⁹⁵ target position was 7.7×10^9 n/s at 1MW [44, 49].

A_γ^{np} was determined from interactions of the polar-¹⁹⁶ ized neutron beam on a 16 l liquid hydrogen (LH₂) tar-¹⁹⁷ get in the parahydrogen ($p\text{-H}_2$) molecular state [45, 50].¹⁹⁸ Scattering from the $S = 0$ $p\text{-H}_2$ molecular ground state¹⁹⁹

preserves neutron polarization for incident neutron energies which fall below the 14.7 meV threshold for spin-flip scattering into the $S = 1$ orthohydrogen ($o\text{-H}_2$) molecular ground state. The $o\text{-H}_2$ fraction $f_{o\text{-H}_2}$, which can flip the neutron spin upon scattering, was minimized by continuously circulating the liquid through a catalytic converter operated at 15.4 K [45]. Because of the long neutron mean free path in $p\text{-H}_2$, only about 43% of the incident neutrons were captured by $p\text{-H}_2$. The rest were scattered by the LH_2 and absorbed by the target vessel made from an aluminum alloy or by ^6Li -loaded neutron absorber wrapped on the outside surface of the vessel. $f_{o\text{-H}_2}$ was monitored periodically with neutron transmission measurements using M1 and M2 [45]. We measured the neutron- $p\text{-H}_2$ scattering cross sections and used that to determine an upper limit of $f_{o\text{-H}_2} < 0.0015$ [45]. With this limit, we estimated the neutron depolarization to be 0.032 ± 0.016 using MCNPX [51] and the cross sections in [52].

γ -rays were detected with an array of 48 cubical CsI(Tl) detectors (sides 15.2 cm) arranged symmetrically in four rings of 12 covering $\approx 3\pi$ sr [43, 53]. The detector array was aligned within 3 mrad to the local magnetic field direction to suppress any mixing of the PV (up-down) asymmetry with the parity-conserving (left-right) asymmetry [54]. The detectors were operated in current mode due to high instantaneous detector rates of $\sim 10^8$ Hz. Scintillation light was converted to a voltage signal using magnetic field insensitive vacuum photodiodes and low-noise amplifiers [43]. The spectral density of the amplifier noise was measured to be much smaller than the shot noise density from γ counting statistics [55, 56]. The ability of the apparatus to detect a PV asymmetry was tested by measuring the large ($\sim 3 \times 10^{-5}$) PV γ asymmetry from polarized slow neutron capture on ^{35}Cl [57–59]. We observed asymmetries consistent with previous work [60].

The prompt signal from the LH_2 target consisted of $\sim 80\%$ γ 's from capture on hydrogen and $\sim 20\%$ γ 's from capture on aluminum. Neutrons that capture on ^{28}Al produce a prompt PV γ cascade, followed by a β -delayed γ ($\tau = 194$ s). The β -delayed signal manifests as a constant pedestal. The prompt PV γ asymmetry in aluminum must be measured separately. The aluminum prompt γ asymmetry was first measured using the same apparatus, replacing the LH_2 target with an aluminum target. The apparatus was then removed to allow for installation of the next experiment ($n\text{-}^3\text{He}$). During data analysis, the importance of constructing the aluminum target from the same material used to fabricate the LH_2 target vessel became clear. So, the apparatus was re-installed to re-measure the aluminum asymmetry. The different aluminum components of the apparatus such as the RFSR windows, cryostat vacuum windows, target vessel entrance and exit windows, and vessel side walls could have different prompt γ asymmetries due to dif-

ferent impurities. To account for this, we built 4 targets from the 4 different components of the apparatus and one target from the window material of the new RFSR. We also built one composite target that incorporated material from each component with mass proportional to their relative yields to the prompt signal, as determined by Monte Carlo calculation [61]. For these measurements, we used the improved DAQ and the high-efficiency RFSR from the $n\text{-}^3\text{He}$ experiment.

Data, analysis, and results. For each neutron pulse, the current-mode signals from each detector were digitized to give 40 time-bins of differential photon yield. These differential yields were summed over a fiducial time interval for which both choppers were open and the neutron polarization was well defined for each spin direction $\uparrow\downarrow$. The neutron polarization was reversed with a 16-step spin sequence (SS) $\uparrow\downarrow\uparrow\downarrow\uparrow\downarrow\uparrow\downarrow\uparrow\downarrow\uparrow\downarrow\uparrow\downarrow\uparrow\downarrow$. A total of 5.9×10^7 SS were accumulated during the LH_2 running. This pattern rejects known 30 Hz beam intensity fluctuations and suppresses drifts up to 3^{rd} order.

The contributions to the detector yields must be understood to determine the PV asymmetries. The β -delayed γ s and small electronic offsets combine to form a pedestal that is nearly time-independent on the scale of a SS. Each CsI(Tl) detector also has a delayed-light, multi-component phosphorescence tail [62] with a typical decay time of 6.7 ± 1.6 ms contributing 1% of the yield in the subsequent pulse (see Figure 2). The tails are assumed to have the same PV and intensity variations as the prompt yields. The asymmetry for detector d is defined in terms of prompt photon yields, Y_d , as $A_d = \frac{(Y_d^\uparrow - Y_d^\downarrow)}{(Y_d^\uparrow + Y_d^\downarrow)}$, but is not measured directly. The measured detector yields contain non-prompt contributions (and delayed light tails) as defined above. These contributions can be determined from “dropped pulses”, in which protons were not sent to the spallation target and the prompt photons are not present in the signal, but non-prompt contributions are (see Figure 2). Three different analyses used information from dropped pulses to properly normalize the asymmetries.

All data for which the apparatus was operating normally were included in the analysis. Roughly 20% of SS were eliminated because of unstable beam power, improper chopper phasing (which impacts the fiducial time window) or RFSR errors. The measured neutron intensity in the polarization-insensitive monitor M1 was used to apply the beam power cuts, which accounted for nearly all of the eliminated data. Figure 3 shows the effect of these cuts on the asymmetry of a typical detector. After cuts were applied, the asymmetry distributions were indistinguishable from Gaussian [63]. The extracted asymmetries determined using three different analyses agreed to within a small fraction of the statistical uncertainties.

The aluminum asymmetry measurements were taken with a different DAQ and RFSR using a simple 30 Hz neutron spin state reversal pattern $\uparrow\downarrow\uparrow\downarrow \dots$, with a total

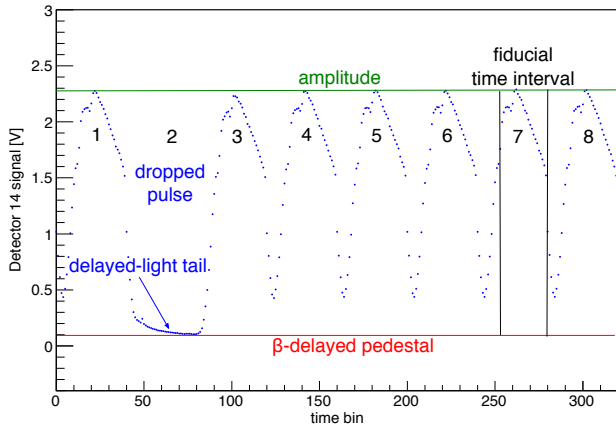


FIG. 2. Plot of a typical detector voltage signal as a function of time-bin for eight 60 Hz neutron pulses. The proton pulse was not delivered to the spallation target in the 2nd pulse resulting in a dropped pulse. The peak yield in the 3rd pulse is 1% low because the phosphorescence tail from the second pulse is missing. The rising (falling) edges of the pulses correspond to the choppers opening (closing). The pedestal from the β -delayed γ s of ^{28}Al is shown. Finally, the fiducial time interval (27 time-bins wide) is shown in pulse seven (time-bins 253 to 279).

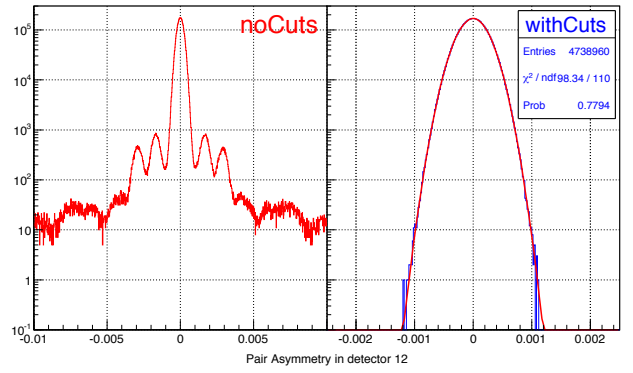


FIG. 3. Histogram of hydrogen asymmetries ($\sim 1/30$ of all the data) for a typical detector before (left) and after (right) the cuts described in the text have been applied. Note the different x-axis scale on the right panel. The distinct side lobes in the uncut data correspond to SS in which one or more dropped pulses occurred.

tions [61, 65] and the covariances were determined from data.

The relationship between the pair asymmetries A_p and the physics asymmetries A_γ becomes

$$A_p = \sum_i P_{tot}^i f_p^i G_p^i A_\gamma^i, \text{ where } P_{tot}^i, f_p^i, G_p^i \text{ and } A_\gamma^i \text{ are the}$$

net polarization factor (beam polarization, target depolarization, and RFSF efficiency), the fractional contribution to the detector yield, the geometric factor, and the γ asymmetry of the i^{th} target component (e.g., hydrogen, aluminum window, etc.) respectively, for detector pair p .

The hydrogen and aluminum asymmetries were simultaneously extracted from a χ^2 minimization scheme using data sets from hydrogen and aluminum targets as well as the corresponding sets of P_{tot}^i , f_p^i , and G_p^i . Three different analyses were consistent in their results. The integrated χ^2 probability for each analysis was 0.73, 0.64, and 0.43. The extracted hydrogen asymmetry is $A_\gamma^{np} = (-3.0 \pm 1.4(\text{stat.})) \times 10^{-8}$ and the extracted aluminum PV asymmetry is $(-12 \pm 3(\text{stat.})) \times 10^{-8}$. The statistical uncertainty is only 15% larger than expected from the neutron beam shot noise [49].

Systematic uncertainties. Table 1 lists the largest systematic uncertainties in our measurement of A_γ^{np} . The variation in thickness of the formed aluminum entrance windows leads to an uncertainty in the fractional yield of prompt aluminum γ s, resulting in a systematic uncertainty in A_γ^{np} of 1×10^{-9} [64]. The targets used to measure the aluminum asymmetry were centered in the detector array, while the aluminum components of the apparatus were located near the upstream end of the detector. We tested our ability to calculate geometric factors for such different geometries by measuring the large Cl asymmetry with targets in the center, front, and back of the detector [60]. The spread in the extracted Cl asymmetries was 3%, which yields an additional uncer-

of 1.5×10^7 SS accumulated. This simple reversal pattern introduced a sensitivity to a 30 Hz neutron intensity modulation of 10^{-4} . Proper normalization of raw detector asymmetries was applied to remove detector dependence from such 30 Hz signals. The information needed to normalize the detector responses was determined from the detector yields in the neighborhood of the dropped pulses [61, 64]. Detector-pair asymmetries were formed from the difference of azimuthally opposing detector asymmetries to extract the physics result. In order to verify that the normalization sufficiently suppressed the 30 Hz modulation, a regression analysis was performed between the beam intensity modulation extracted from M1 signals and the pair asymmetries. The slope of this regression was consistent with zero.

The differential cross section for the direction of the capture γ s with respect to the spin direction is $\frac{d\sigma}{d\Omega} \sim 1 + A_\gamma \vec{k}_\gamma \cdot \vec{s}_n$, neglecting parity-conserving contributions. Correcting for the finite geometry of the beam, target, and detectors requires a Monte Carlo calculation of the energy-weighted values of the average scalar product $\vec{k}_\gamma \cdot \vec{s}_n$ for each detector, denoted “geometric factors”. The geometric factors are calculated for all γ rays from simulated neutron capture in the target, target vessel, and its surrounding shielding which deposit energy in a detector element. Compton scattering causes a single γ to deposit energy in more than one detector leading to correlations between energy depositions in different detectors. These correlations lead to non-diagonal uncertainty covariance matrices. The geometric factors were calculated using GEANT4 and MCNPX simula-

TABLE I. Dominant sources of systematic uncertainty and their contributions to A_γ^{np} .

Source	Contribution
Prompt Al γ s: window thickness	1×10^{-9}
Prompt Al γ s: geometric factors	7×10^{-10}
^{28}Al bremsstrahlung	$< 9 \times 10^{-11}$
False electronic asymmetry (LEDs off)	$< 1 \times 10^{-9}$
False electronic asymmetry (LEDs on)	$< 1 \times 10^{-9}$
Remaining systematic uncertainty [43]	$< 3 \times 10^{-10}$
Total	$< 2 \times 10^{-9}$

325 tainty from the contribution of prompt aluminum γ 's of
326 7×10^{-10} .

327 Another systematic uncertainty arises from
328 bremsstrahlung γ 's from the β -decay of polarized
329 ^{28}Al . The ^{28}Al ground state β -decays to the first excited
330 state of ^{28}Si and the direction of the β and subsequent
331 bremsstrahlung γ 's are correlated with the polarization
332 direction by the PV β asymmetry parameter, which is
333 assumed to have its maximum possible value of unity.
334 The bremsstrahlung yield was calculated from recent
335 measurements [66]. The spin-lattice relaxation of the
336 polarized aluminum nuclei at room and LH₂ tempera-
337 tures and the effects of the different polarization reversal
338 patterns were included. The estimated systematic
339 uncertainty was below 0.9×10^{-10} .

340 All other systematic effects discussed in [43] were re-
341 considered and their limits were either unchanged or
342 slightly reduced. False electronic asymmetries were pe-
343 riodically measured with the neutron beam off and light
344 emitting diodes (LEDs) illuminating the scintillator crys-
345 tals (LED ON) or not (LED OFF). False asymmetries in
346 both cases were less than 1×10^9 .

347 Multiplicative corrections are applied to the data to
348 account for geometric factors and neutron polarization.
349 These include the uncertainties in the neutron depo-
350 larization by orthohydrogen (1.6%), geometric factors
351 (3%), beam polarization (0.5%), and spin flipper effi-
352 ciency (0.5%). The relative uncertainties of the three
353 analysis methods were estimated to be 1% [49]. The com-
354 bined uncertainty from these corrections is 3.6%, which
355 is negligible when added in quadrature with the 47% sta-
356 tistical uncertainty in the PV asymmetry.

357 The final result for the hydrogen asymmetry is $A_\gamma^{np} =$
358 $(-3.0 \pm 1.4(\text{stat.}) \pm 0.2(\text{sys.})) \times 10^{-8}$. This is consistent
359 with the statistics-limited Phase 1 result and surpasses
360 the precision of [67] which was unable to resolve A_γ^{np} .

361 *Discussion and Conclusion.* We can extract a value
362 of h_π^1 from the measured asymmetry because the heavy
363 meson couplings enter the expression of A_γ^{np} with very
364 small coefficients. Hyun *et al.* [31] and Liu [30] give ex-
365 pansion of A_γ^{np} in the meson-exchange picture using the
366 AV18 NN potential: $A_\gamma^{np} = -0.117h_\pi^1 - 0.001h_\rho^1 + 0.002h_\omega^1$
367 and $A_\gamma^{np} = -0.111h_\pi^1 - 0.001h_\rho^1 + 0.002h_\omega^1$, respec-

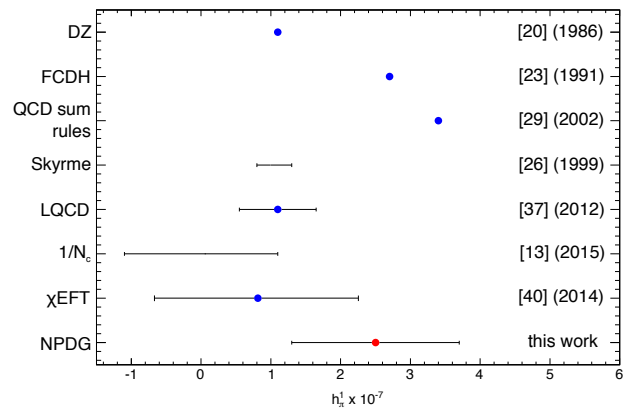


FIG. 4. h_π^1 from theoretical estimates or calculations (blue) and this work (red).

tively. We adopt the average of these two expansions, $A_\gamma^{np} = -0.114h_\pi^1 - 0.001h_\rho^1 + 0.002h_\omega^1$. The RMS theoretical uncertainty in this procedure is 3%, which is negligible compared to the statistical uncertainty. Neglecting heavy-meson terms, which contribute less than 1% of A_γ^{np} in the DDH reasonable range [1], we obtain $h_\pi^1 = (2.6 \pm 1.2(\text{stat.}) \pm 0.2(\text{sys.})) \times 10^{-7}$. Our value for A_γ^{np} gives the pionless EFT coupling constant $C^{^3S_1 \rightarrow ^3P_1}/C_0 = (-7.4 \pm 3.5(\text{stat.}) \pm 0.5(\text{sys.})) \times 10^{-11} \text{ MeV}^{-1}$ [7]. Since A_γ^{np} only depends on h_π^1 and ^{18}F P_γ contains all of the $\Delta I = 1$ contributions, we can eliminate h_π^1 and find a constraint on the heavy mesons to be $0.4 h_\rho^1 + 0.6 h_\omega^1 = 8.5 \pm 5.0$, which is consistent with recent theoretical estimates [13, 16].

Figure 4 shows an overview of theoretical estimates and this work's extraction of h_π^1 . We report the most precise and direct determination of h_π^1 in a few-body system without atomic or nuclear corrections, and it is the best constraint for future investigation of the HWI. Additional theoretical and experimental work in exactly calculable few-body systems is needed to establish a complete determination of the HWI.

We gratefully acknowledge the support of the U.S. Department of Energy Office of Nuclear Physics through grants DE-AC52-06NA25396, DE-FG02-03ER41258, DE-SC0014622, DE-AC-02-06CH11357, DE-AC05-00OR22725, and DE-SC0008107, the US National Science Foundation through grants PHY-1306547, PHY-1306942, PHY-1614545, PHY-0855584, PHY-0855610, PHY-1205833, PHY-1506021, PHY-1205393, and PHY-0855694, PAPIIT-UNAM grants IN110410, IN11193, and IG1011016, CONACYT grant 080444, the Natural Sciences and Engineering Research Council of Canada (NSERC), and the Canadian Foundation for Innovation (CFI). This research used resources of the Spallation Neutron Source of Oak Ridge National Laboratory, a DOE Office of Science User Facility. J. Fry, R. C. Gillis, J. Mei, W. M. Snow, and Z. Tang acknowledge support

- 406 from the Indiana University Center for Spacetime
407 Symmetries. S. Schröder acknowledges support from the
408 German Academic Exchange Service (DAAD).
-
- 409 [1] B. Desplanques, J. F. Donoghue, and B. R. Holstein,
410 Ann. Phys. **124**, 449 (1980).
411 [2] C. A. Barnes *et al.*, Phys. Rev. Lett. **40**, 840 (1978); M.
412 Bini *et al.*, Phys. Rev. Lett. **55**, 795 (1985); G. Ahrens
413 *et al.*, Nucl. Phys. A**390**, 496 (1982); S. A. Page *et al.*,
414 Phys. Rev. C **35**, 1119 (1987).
415 [3] G. S. Danilov, Phys. Lett. **18**, 40 (1965).
416 [4] G. S. Danilov, Sov. J. Nucl. Phys. **14**, 443 (1972).
417 [5] S.-L. Zhu, C. Maekawa, B. Holstein, M. Ramsey-Musolf,
418 and U. van Kolck, Nucl. Phys. A**748**, 435 (2005).
419 [6] D. R. Phillips, M. R. Schindler, and R. P. Springer, Nucl.
420 Phys. A**822**, 1 (2009).
421 [7] M. Schindler and R. Springer, Prog. Part. Nucl. Phys.
422 **72**, 1 (2013).
423 [8] G. t Hoof, Nucl. Phys. B **72**, 461 (1974).
424 [9] E. Witten, Nucl. Phys. B **160**, 57 (1979).
425 [10] E. Jenkins, Ann. Rev. Nucl. Part. Sci. **48**, 81 (1998).
426 [11] T. D. Cohen and B. A. Gelman, Phys. Rev. C **85**, 024001
427 (2012).
428 [12] T. DeGrand and Y. Liu, Phys. Rev. D **94**, 034506 (2016).
429 [13] D. R. Phillips, D. Samart, and C. Schat, Phys. Rev. Lett.
430 **114**, 062301(2015).
431 [14] D. Samart, C. Schat, M. R. Schindler, and D. R. Phillips,
432 Phys. Rev. C **94**, 024001 (2016).
433 [15] M. R. Schindler, R. P. Springer, and J. Vanasse, Phys.
434 Rev. C **93**, 025502 (2016).
435 [16] S. Gardner, W. C. Haxton, and B. R. Holstein, Ann. Rev.
436 Nucl. Part. Sci. **67**, 69 (2017).
437 [17] E. G. Adelberger and W. C. Haxton, Ann. Rev. Nucl.
438 Part. Sci. **35**, 501 (1985); M. J. Ramsey-Musolf and S.
439 A. Page, Ann. Rev. Nucl. Part. Sci. **56**, 1 (2006).
440 [18] W. C. Haxton and B. R. Holstein, Prog. Part. Nucl. Phys.
441 **71**, 185 (2013).
442 [19] V. Khatsimovsky, Sov. J. Nucl. Phys. **42**, 781 (1985).
443 [20] V. M. Dubovik and S. V. Zenkin, Ann. Phys. **172**, 100
444 (1986).
445 [21] N. Kaiser and U.-G. Meissner, Nucl. Phys. A**489**, 671
446 (1988).
447 [22] N. Kaiser and U.-G. Meissner, Nucl. Phys. A**510**, 759
448 (1990).
449 [23] G.B. Feldman, *et al.*, Phys. Rev. C **43**, 863 (1991).
450 [24] E. Henley, W. Hwang, and L. Kisslinger, Phys. Lett.
451 **B367**, 21 (1996).
452 [25] E. Henley, W. Hwang, and L. Kisslinger, Phys. Lett.
453 **B440**, 449 (1998).
454 [26] U.-G. Meisser and H. Weigel, Phys. Lett. B **447**, 1 (1999).
455 [27] S.-L. Zhu, S. Puglia, B. R. Holstein, and M. Ramsey-
456 Musolf, Phys. Rev. D **63**, 033006 (2001).
457 [28] M. J. Savage, Nucl. Phys. A **695** (2001).
458 [29] G. Lobov, Physics of Atomic Nuclei **65**, 3 (2002).
459 [30] C.-P. Liu, Phys. Rev. C **75**, 065501 (2007) and private
460 communication.
461 [31] C. H. Hyun, S. Ando, and B. Desplanques, Phys. Lett.
462 **B 651**, 257 (2007).
463 [32] C. H. Hyun, B. Desplanques, S. Ando, and C.-P. Liu,
464 Mod. Phys. Lett. A **23**, 2293 (2008).
465 [33] B. Desplanques, C.H. Hyun, S. Ando, and C.-P. Liu,
466 Phys. Rev. C **77**, 064002 (2008).
467 [34] D. Gazit and H.-U. Yee, Phys. Lett. **B670**, 154 (2008).
468 [35] M.R. Schindler and R.P. Springer, Nucl. Phys. A **846**,
469 51 (2010).
470 [36] H.-J. Lee, C. H. Hyun, and H.-C. Kim, Phys. Lett. **B713**,
471 439 (2012).
472 [37] J. Wasem, Phys. Rev. C **85**, 022501(R) (2012).
473 [38] J. de Vries, U.-G. Meissner, E. Epelbaum and N. Kaiser,
474 Eur. Phys. J. A **49**, 149 (2013).
475 [39] M. Viviani, A. Baroni, L. Girlanda, A. Kievsky, L. E.
476 Marcucci, and R. Schiavilla, Phys. Rev. C **89**, 064004
477 (2014).
478 [40] J. de Vries, *et al.*, Eur. Phys. J. A **50**, 108 (2014).
479 [41] J.de Vries, N.Li, U. G. Meissner, A. Nogga, E. Epelbaum
480 and N. Kaiser, Phys. Lett. B **747**, 299 (2015).
481 [42] X. Feng, F.-K. Guo, and C.-Y. Seng, Phys. Rev. Lett.
482 **120**, 181801 (2018).
483 [43] M. T. Gericke *et al.*, Phys. Rev. C **83**, 015505 (2011).
484 [44] N. Fomin *et al.*, Nucl. Instr. Meth A**773**, 45 (2015).
485 [45] K. B. Grammer *et al.*, Phys. Rev. B **91**, 180301 (2015).
486 [46] M. Musgrave *et al.*, Nucl. Instr. Meth A **895**, 19 (2018).
487 [47] S. Balascuta *et al.*, Nucl. Instr. Meth A**671**, 137 (2012).
488 [48] P.-N. Seo *et al.*, Phys. Rev. ST Accel. Beams **11**, 084701
489 (2008).
490 [49] J. Fry, PhD thesis, Indiana University (2015).
491 [50] S. Santra *et al.*, Nucl. Instr. Meth A**620**, 421 (2010).
492 [51] D. Pelowitz (ed.), *MCNPIX Users Manual*, Version
493 2.7.0, Los Alamos National Laboratory, LA-CP-11-00438
494 (2011).
495 [52] J. Young and J. Koppel, Phys. Rev 135 (3A), 603 (1964).
496 [53] M. T. Gericke *et al.*, Nucl. Instr. Meth A **450**, 21 (2005).
497 [54] A. Csoto, B. Gibson, and G. L. Payne, Phys. Rev. C **56**,
498 631 (1997).
499 [55] M. T. Gericke *et al.*, Nucl. Instr. Meth A**540**, 328 (2005).
500 [56] W. S. Wilburn, J.D. Bowman, S.I. Penttila, and M.T.
501 Gericke. Nucl. Inst. Meth. A **540**, 180 (2005).
502 [57] V. A. Vesna, *et al.*, JETP Lett. **36**, 209 (1982).
503 [58] M. Avenier *et al.*, Nucl. Phys. A**436**, 83 (1985).
504 [59] G.S. Mitchell *et al.*, Nucl. Instr. Meth. A**521**, 468 (2004).
505 [60] N. Fomin *et al.*, to be submitted to Phys. Rev. C (2018).
506 [61] D. Blyth, PhD thesis, Arizona State University (2016).
507 [62] C.L. Woody, *et al.*, IEEE Transactions on Nuclear Sci-
508 ence, 39, 4, 524-531 (1992).
509 [63] J. Fry *et al.*, Hyperf. Int. **238**, 11 (2017).
510 [64] D. Blyth *et al.*, to be submitted to Phys. Rev. C (2018).
511 [65] K. B. Grammer *et al.*, Nucl. Instr. Meth A**903**, 21 (2018).
512 [66] L. Pandola, C. Andenna, and B. Caccia, Nucl. Instr.
513 Meth. B**350**, 41 (2015).
514 [67] J. F. Caviagnac *et al.*, Phys. Lett. B **67**, 148 (1977).
515 [68] C. Hyun, S. Lee, J. Haidenbauer, S. Hong, Eur. Phys. J.
516 A **24**, 129135 (2005).